Improved Synthesis of Hollow Fiber SSZ-13 Zeolite Membranes for High-Pressure CO2/CH4 Separation

Peng, Xingyu; Chen, Lingjie; You, Lekai; Jin, Yang; Zhang, Chun; Ren, Shengyuan; Kapteijn, Freek; Wang, Xuerui; Gu, Xuehong

DOI
10.1002/anie.202405969

Publication date
2024

Document Version
Final published version

Published in
Angewandte Chemie - International Edition

Citation (APA)
Peng, X., Chen, L., You, L., Jin, Y., Zhang, C., Ren, S., Kapteijn, F., Wang, X., & Gu, X. (2024). Improved Synthesis of Hollow Fiber SSZ-13 Zeolite Membranes for High-Pressure CO2/CH4 Separation. *Angewandte Chemie - International Edition*, *63*(31), Article e202405969. https://doi.org/10.1002/anie.202405969

How to cite: Angew. Chem. Int. Ed. 2024, e202405969
doi.org/10.1002/anie.202405969

VIP Gas Separation Very Important Paper

Improved Synthesis of Hollow Fiber SSZ-13 Zeolite Membranes for High-Pressure CO_2/CH_4 Separation

Xingyu Peng, Lingjie Chen, Lekai You, Yang Jin, Chun Zhang, Shengyuan Ren, Freek Kapteijn, Xuerui Wang, and Xuehong Gu**

Abstract: High-silica CHA zeolite membranes are highly desired for natural gas upgrading because of their separation performance in combination with superior mechanical and chemical stability. However, the narrow synthesis condition range significantly constrains scale-up preparation. Herein, we propose a facile interzeolite conversion approach using the FAU zeolite to prepare SSZ-13 zeolite seeds, featuring a shorter induction and a longer crystallization period of the membrane synthesis on hollow fiber substrates. The membrane thickness was constant at ~3 μm over a wide span of synthesis time (24-96 h), while the selectivity (separation efficiency) was easily improved by extending the synthesis time without compromising permeance (throughput). At 0.2 MPa feed pressure and 303 K, the membranes showed an average CO_2 permeance of $(5.2\pm0.5)\times10^{-7}$ mol m^{-2} s^{-1} Pa^{-1} (1530 GPU), with an average CO_2/CH_4 mixture selectivity of 143 ± 7. Minimal defects ensure a high selectivity of 126 with a CO_2 permeation flux of 0.4 mol m^{-2} s^{-1} at 6.1 MPa feed pressure, far surpassing requirements for industrial applications. The feasibility for successful scale-up of our approach was further demonstrated by the batch synthesis of 40 cm-long hollow fiber SSZ-13 zeolite membranes exhibiting CO_2/CH_4 mixture selectivity up to 400 (0.2 MPa feed pressure and 303 K) without using sweep gas.

Introduction

Zeolites are a group of crystalline and microporous materials that are generally constructed by TO_4 tetrahedra (T = Si, Al, etc.).[1] Their features of uniform pores with molecular dimension, high porosity, and excellent thermal and chemical stability offer great potential as membrane materials.[2] Extensive efforts have been put into modulating membrane microstructure and understanding transport mechanisms.[3] However, the NaA zeolite membrane is the only commercialized one on an industrial scale for organic solvent dehydration.[4] The small-pore zeolite membranes DDR and CHA demonstrated exciting performance towards the gas separation of CO_2/CH_4,[5] CO_2/Xe,[6] Kr/Xe,[7] and SO_2/NO_2.[8] However, the practical applications remain extremely challenging nowadays because of the low permeation flux (<0.2 mol m^{-2} s^{-1})[9] and the narrow range of synthesis conditions for reproducible scaling-up.

High-silica CHA (Si/Al > 5, also named SSZ-13[10]) zeolite membranes are typically prepared using the secondary growth method. The pristine crystals serving as seeds should be small and mono-dispersed for a thin selective layer to improve permeation flux.[11] The thickness of the first SSZ-13 zeolite membranes, induced by micron-sized seeds (2-5 μm), ranged from 10-40 μm.[12] To hydrothermally synthesize small seeds, modifications have been made to gel compositions (*e.g.*, TMAdaOH,[13] water,[14] hydrofluoric acid[15] content) and synthesis procedures (*e.g.*, solution aging, time, temperature),[16] but undesired big crystals were still present due to the intergrowth. Hedlund *et al.*[15,17] proved the efficiency of fluoride synthesis to reduce the membrane thickness to 0.45-1.3 μm. Because hydrofluoric acid can cause lingering disease in humans, the synthesis procedure and the waste disposal are complex and cost-intensive. Kosinov *et al.*[18] synthesized 4-6 μm-thick membranes using ball-milled seeds in a fluorine-free solution. However, the seed yield was limited to 20 % by the complicated ball-milling and centrifuge cycles.[19] Furthermore, the seeds are readily contaminated with impurities from the jar/balls although the effect on membrane formation is unclear.

Secondary growth involves two steps of seeding and hydrothermal synthesis, leading to a low yield of 30-70 % for gas-selective zeolite membranes.[20] Recently, Nair *et al.*[6] pioneered a single-step method for producing high-quality SSZ-13 zeolite membranes called viscosity-confined dry gel conversion. This method not only offers the advantage of minimum chemical use but also has the potential to improve reproducibility.[21] To reduce fabrication costs, researchers also explored substituting the expensive organic structure-directing agent (OSDA) of *N,N,N*-trimethyl-1-adamantammonium hydroxide (TMAdaOH) with a cheaper one (*e.g.*, tetraethylammonium hydroxide)[22] or using organic tem-

[*] X. Peng, L. Chen, L. You, Y. Jin, Dr. C. Zhang, S. Ren, Prof. Dr. X. Wang, Prof. Dr. X. Gu
State Key Laboratory of Materials-Oriented Chemical Engineering, College of Chemical Engineering, Nanjing Tech University, No. 30 Puzhu South Road, Nanjing 211816, P. R. China
E-mail: x.wang@njtech.edu.cn
xhgu@njtech.edu.cn
Prof. Dr. F. Kapteijn
Chemical Engineering Department, Delft University of Technology, Van der Maasweg 9, Delft 2629 HZ, The Netherlands
L. Chen, Prof. Dr. X. Wang, Prof. Dr. X. Gu
Quzhou Membrane Material Innovation Institute
No. 99 Zheda Road, Quzhou 324000, P. R. China

plate-free synthesis.[23] Zhou and co-workers developed SSZ-13 zeolite membranes using 7-,[9b] 19-,[16] and 61-channel[24] monoliths as the substrates to increase module packing density. Despite important achievements, all these attempts have focused on the synthesis of short membranes (*e.g.*, 5-9 cm).[6,9b,16,21,24-25] The synthesis of long SSZ-13 zeolite membranes for gas separation is, however, rarely explored.[26]

Herein, a wide span of synthesis times was explored to synthesize SSZ-13 zeolite membranes by adopting the seeds prepared by an interzeolite conversion method. The SSZ-13 crystals serving as seeds were hydrothermally synthesized using commercial FAU zeolite as the sole Si/Al source and TMAdaOH as OSDA. Four-channel hollow fibers were used as the substrates because of their superior mechanical strength and commercially favorable packing density. The evolution of the dip-coated seeds layer was tracked by varying synthesis time from 2 h to 96 h. The optimized synthesis condition was also used to scale up the membranes with a length of 40 cm. The improved reproducibility and appealing performance were well demonstrated by the scalable batch synthesis of nine membranes for high-pressure CO_2/CH_4 mixture separation.

Results and Discussion

High-silica CHA Zeolite Membrane Synthesis

The SSZ-13 zeolite seeds named FAU-CHA were prepared by interzeolite conversion of FAU zeolite.[27] No diffraction peak assigned to FAU zeolite was identified from the powder X-ray diffraction (PXRD) patterns (Figure 1a), indicating a complete transition. They showed a typical cubic morphology (Figure S1) and an average particle size of 210 nm (Figure S2). The yield was up to 91.2 % based on the FAU amount, proving an efficient approach to scale up. The crystals packed tightly to form a homogeneous layer on the substrates after dip-coating in 0.5 wt % aqueous suspensions (Figure 1b). No crystals were observed inside the substrate (Figure S4) even though their particle size is smaller than the pore size of the substrate (300 nm). Well-intergrown and continuous membranes formed after hydrothermal synthesis of 96 h. Both surface grain size and membrane thickness were around 2.8 μm (Figure 1c-d), indicating the membrane seems to be composed of a mono-layer of well-intergrown crystals. The thickness is only one-third of the membranes synthesized from OH-CHA seeds.[28] An intermediate layer formed on 1.0 wt % suspension seeded substrate after membrane synthesis (Figure S5), which would cause weak adhesion and intercrystalline defects during pressure-driven gas separation (Table S1). Interestingly, the surface grain size (2.8 ± 0.5 μm) is almost the same as the membrane thickness (2.7 μm) as well.

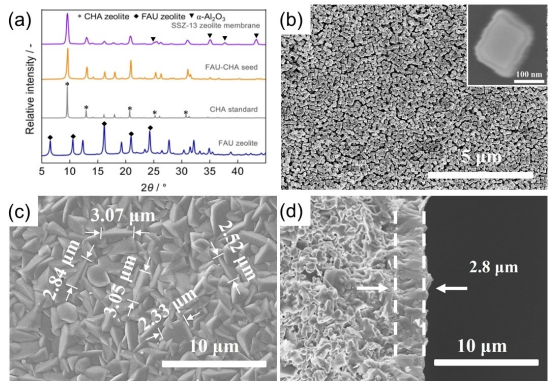

Figure 1. Characterization of the seeds and the corresponding membranes. (a) PXRD patterns. CHA standard XRD pattern was cited from International Zeolite Association. (b) Surface SEM image of seed layer after dip-coating with 0.5 wt % suspension; Inset: Magnified image of seed crystal. (c-d) Surface and cross-sectional SEM images of the membrane synthesized at 433 K for 96 h.

Zeolite Membrane Formation Mechanism

High-silica CHA zeolite membranes were further synthesized for various periods to track the membrane formation. After hydrothermal synthesis of 2 h, the typical cubic crystals were wrapped with some fuzzy material, probably amorphous silica (Figure S6). This should be the silica species for zeolite growth, which are generally formed at the initial stage of crystal growth.[29] The seeds grew up to 0.42 ± 0.06 μm for 6 h but did not show intergrowth (Figure S7a, d). The crystals gradually intergrew to form a 1.5 μm-thick membrane after hydrothermal synthesis of 10 h (Figure S7b, e). The membrane thickness further increased to 1.9 μm for 18 h (Figure S7f). Interestingly, the membrane morphology regardless of surface grain size and thickness kept constant once synthesis time was extended beyond 24 h (Figure S7g-l). The membrane thickness and the ratio to surface grain size with synthesis time are plotted in Figure 2a. Indeed, the thickness increased and levelled off at ~3.0 μm after 24 h. Meanwhile, the ratio of thickness to grain size gradually decreased and stabilized around one. We defined this point as a "critical time" for the well intergrowth to form high-quality membranes. On the other hand, the conventional OH-CHA seeds, with similar initial particle size (*ca.* 200 nm), leads to a steady increase in the membrane thickness.[16,28a] To confirm this unusual phenomenon, three more membranes were synthesized at each period of 24 h, 48 h, 72 h, and 96 h for thickness examination (Figure S8). Indeed, all the membranes showed a thickness of approximately 3.0 μm, demonstrating a reproducible synthesis procedure.

The quality of all the membranes was evaluated by equimolar CO_2/CH_4 mixture separation (Figure 2b). Even though the average selectivity of the membranes synthesized for 24 h was comparable with our earlier work (77 *vs.* 48),[28b] a large variation between 29 and 113 was observed. While a consistent performance is highly desired for the scalable synthesis. Once secondary growth was extended beyond the "critical time" of 24 h, not only selectivity improved but also the variation gradually diminished. Especially all four membranes synthesized for 72 h showed a selectivity

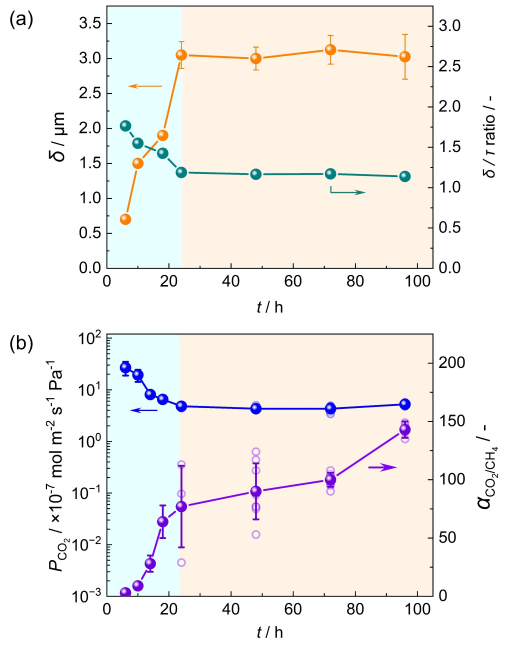

Figure 2. Effect of synthesis time (t) on membrane morphology and separation performance. (a) Membrane thickness (δ) and the ratio to surface grain size (τ); (b) Binary CO_2/CH_4 mixture separation performance at 0.2 MPa feed pressure and 303 K. Numerical data can be found in Table S1.

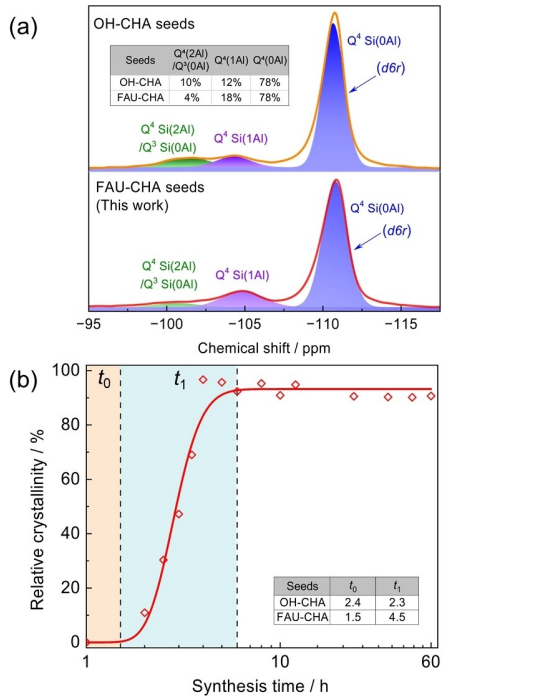

Figure 3. Characterization of the seeds. (a) ^{29}Si MAS NMR. (b) Crystallization curve of high-silica CHA zeolite induced by FAU-CHA seeds. t_0: induction period; t_1: crystallization period. The raw data for OH-CHA seeds are shown in Figure S11.

approaching 100. Both improved selectivity and smaller variation were further obtained on the membranes synthesized for 96 h, wherein the selectivity ranged from 135 to 149. Interestingly, CO_2 permeance was more or less the same at approximately 5.0×10^{-7} mol m^{-2} s^{-1} Pa^{-1} regardless of synthesis time, which is almost two-fold higher than the one of OH-CHA seeds induced membranes.[28a] This is attributed to the identical and thinner membrane. The selectivity was also constant for the membranes produced using a 1.0 wt % seed suspension even though the value was reduced to ~80 (Table S1). These results demonstrate that the reproducibility is significantly improved by the facile extension of synthesis time. This provides a less restricted condition for highly CO_2-selective zeolite membrane synthesis, attractive for scaled-up production.

To get more insights into zeolite membrane formation, the Si environments of the seeds (Figure S9) were investigated using ^{29}Si NMR.[27,30] CHA-type zeolite has only one crystallographically inequivalent T-site (constructing *d6r*[31]), which accounts for the chemical shift at −111 ppm (Si(0Al), Figure 3a). The resonance at −105 ppm can be assigned to Q^4 sites (Si(1Al)). No sign of octahedral Al was observed from ^{27}Al NMR, indicating a more regular structure of FAU-CHA seeds than OH-CHA seeds (Figure S10). The resonance at −101 ppm should stem from the defect sites (Q^4(2Al) or Q^3(0Al)). Interestingly, the defect fraction was two-fold less for our FAU-CHA seeds (4 % *vs.* 10 %). Both seeds were further used to synthesize high-silica CHA zeolite at different times and then recovered for relative crystallinity determination.[32] The kinetic crystallization curve was divided into induction period (t_0) and crystallization period (t_1, Figures 3b, S11). The t_0 decreased by 40 % compared to the traditional one (1.5 h *vs.* 2.4 h). On the contrary, the t_1 extended to 4.5 h almost two times longer. The longer crystallization period allowed a better self-healing of the non-selective pores, *e.g.* by Ostwald-ripening.[33]

Gas Separation Performance Evaluation

The single gas permeation was further tested using light gas molecules with different kinetic diameters. The permeance decreased following the sequence of $CO_2 > H_2 > N_2 > CH_4$ (Figure S13). CO_2 permeance was 5 times higher than that of H_2 even though the kinetic diameter was larger. The preferential adsorption is a reasonable explanation.[34] The ideal CO_2/CH_4 selectivity was comparable and even higher than the reported ones (254 *vs.* 20-133).[18,35] The ideal selectivity was 7 for N_2/CH_4 and 35 for CO_2/N_2 much higher than Knudsen selectivity (Table S3). These results indicate promising applications for natural gas upgrading, CO_2-EOR,[36] nitrogen removal from natural gas,[37] and CO_2 capture from flue gas.[37-38]

The single and mixed gas permeation of CO_2 and CH_4 as a function of temperature and pressure are given in Figure 4. The CO_2 permeance was 8.6×10^{-7} mol m^{-2} s^{-1} Pa^{-1} (2530 GPU) at 303 K then monotonically decreased with temperature up to 453 K (Figure 4a). This is a typical phenomenon of the surface diffusion mechanism,[39] where gas permeation is dominated by adsorption. The CH_4

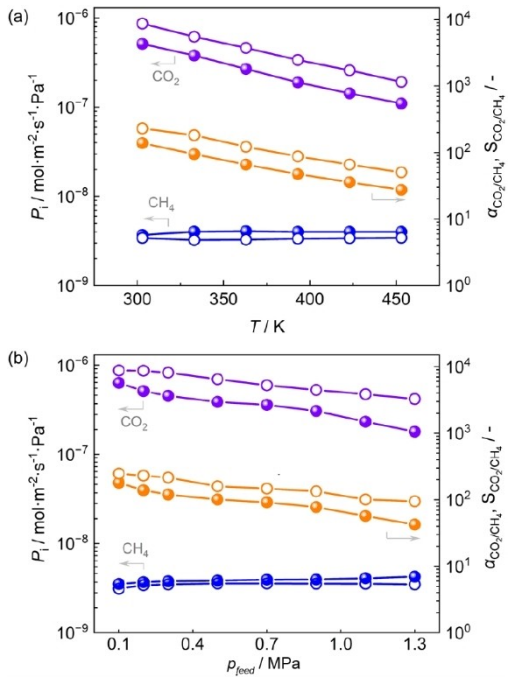

Figure 4. CO_2/CH_4 separation performance. (a) Temperature-dependent permeance at 0.2 MPa feed pressure. (b) Pressure-dependent permeance at 303 K. The membrane effective length was 5 cm and the feed flow rate was 150 mL min^{-1}. The permeate was atmospheric pressure and Ar was used as sweep gas. Open symbols: Single gas permeation; Closed symbols: Equimolar mixture separation.

permeance very weakly increased, indicating that the diffusivity activation energy is slightly larger than its heat of adsorption, similar to DD3R zeolite membranes.[40] The pure CH_4 permeance increased by ~10 % with pressure up to 1.3 MPa (Figure 4b). The increased CH_4 permeance with pressure is explained by the increased diffusivity with loading.[41]

The equimolar CO_2/CH_4 mixture separation performance showed the mutual influence of the permeating species. The CO_2 permeance was 27 % lower than its single component permeance at 0.1 MPa and 57 % lower at 1.3 MPa (Figure 4b). However, the CH_4 permeance showed slightly higher values, resulting in lower mixture selectivity, even though IAST adsorption selectivity of CO_2 over CH_4 predicts an increase with pressure,[18] the CH_4 loading increased by 3-fold (Figure S14). The more CH_4 molecules are accommodated inside the CHA cages, the stronger slowing down effects on CO_2 permeation.[42] On the other hand, the CH_4 transport was sped up leading to a higher permeance than the single component one. This explained well why CO_2/CH_4 mixture selectivity was always lower than the ideal one. Apart from pressure also concentration polarization affects selectivity. Increasing the flow rate to 1 L min^{-1} increased the mixture selectivity to 168 at 0.1 MPa (Figure S15, Figure S16), reducing the stage-cut to merely 3.1 %. The selectivity was still as high as 126 at a feed pressure of 6.1 MPa with a CO_2 permeance of 1.7×10^{-7} mol m^{-2} s^{-1} Pa^{-1} (Figure S15). The CO_2 permeation flux reached 0.4 mol m^{-2} s^{-1}, two times higher than other CHA-type tubular SAPO-34[9a] and 7-channel SSZ-13[9b] zeolite membranes. Furthermore, the membrane is mechanically stable as evidenced by the identical performance when depressurizing back to 0.2 MPa (Figure S15). Irreversible structural changes due to compression and plasticization as occurs in polymeric membranes are absent.[43]

Reliable Scaling-Up of Membrane Synthesis

The most challenging issue is the scale-up synthesis of zeolite membranes for high-pressure gas separation.[16,24, 26a, 44] Here, the scaled-up synthesis of nine 40 cm-long membranes was carried out in one batch to verify the feasibility of our approach (Figure 5a). Both the surface grain size and membrane thickness are approximately 3 μm (Figure 5b-c). The membrane quality was evaluated by an equimolar CO_2/CH_4 mixture at 0.3 MPa and feed flow rate of 1000 mL min^{-1} instead of 150 mL min^{-1} since the effective membrane area increased by 7-fold. The nine membranes showed CO_2 permeance of $(5.9\pm1.1)\times10^{-7}$ mol m^{-2} s^{-1} Pa^{-1} and CO_2/CH_4 selectivity of 181 ± 26 (Figure 5d). Both the texture and separation performance were almost identical to the short ones.

To evaluate the feasibility for practical application, the 40 cm-long membranes were also tested under various feed

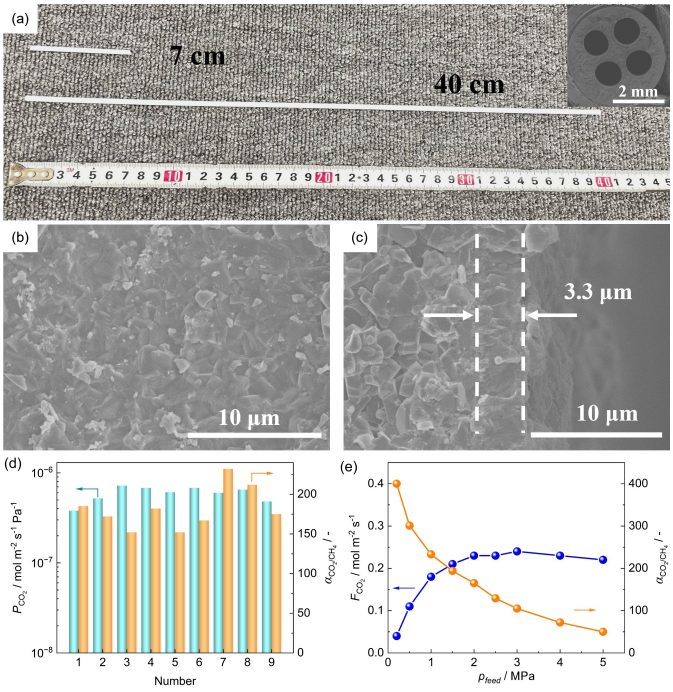

Figure 5. Scale-up synthesis of high-silica CHA zeolite membranes. (a) Photo of short and long membranes. Inset: cross-sectional of the membrane. (b-c) SEM images of the surface and cross-sectional of the long membrane. (d) Equimolar CO_2/CH_4 separation performance of 40 cm-long membranes at a feed flow rate of 1 L min^{-1}. Numerical values measured at 0.3 MPa and 303 K are shown in Table S4. (e) High-pressure CO_2/CH_4 separation performance at a feed flow rate of 4 L min^{-1}. CO_2 concentration in the permeate is shown in Figure S18.

pressures. The permeate was atmospheric pressure and without using sweep gas (Figure S17). Similarly, to the short membranes, both CO_2 permeance and CO_2/CH_4 selectivity monotonously decreased with pressure (Figure S18a). The selectivity was 400 at 0.2 MPa and still up to 50 at a feed pressure of 5.0 MPa, which corresponds to a CO_2 concentration of 96.8 % in the permeate stream (Figure S18b). Their performance surpassed the other membranes synthesized in fluorine-free solution[9b] and is comparable with the ones synthesized from fluorine solution.[26a] The CO_2 permeation flux gradually increased with pressure and levelled off at 0.25 $mol\,m^{-2}s^{-1}$ beyond 2.0 MPa (Figure 5e). We attribute this to the high stage-cut (~34.1 %) and competitive adsorption (Figure S19) under the applied conditions. The result indicates the optimized operation pressure should be <2.0 MPa to achieve maximum permeation flux and minimum compression energy consumption for the practical application.

Conclusion

Mono-dispersed high-silica CHA zeolite with an average particle size of 210 nm was synthesized by the interzeolite conversion of FAU zeolite. The novel FAU-CHA seeds significantly improved the crystal intergrowth, leading to a monocrystal-thick high-silica CHA zeolite membrane. All the membrane thickness was consistent at about 3 μm once the secondary growth was beyond the critical time of 24 h. The intercrystalline pores gradually self-healed by facile extension of the synthesis time, leading to the improved reproducibility of the high-quality membranes. The batch-synthesized membranes showed CO_2 permeance of $(5.2\pm0.5)\times10^{-7}$ $mol\,m^{-2}s^{-1}Pa^{-1}$ and CO_2/CH_4 selectivity of 143 ± 7 at 0.2 MPa and 303 K. Because of the well-intergrown zeolite crystals within the membranes, the CO_2/CH_4 selectivity was up to 126 at the feed pressure of 6.1 MPa, far surpassing the requirements of industrial applications. The feasibility of scaling-up was further demonstrated by the synthesis of 40 cm-long membranes. At 0.2 MPa feed pressure and 303 K, the membranes exhibit CO_2/CH_4 mixture selectivity up to 400 without using sweep gas. Our approach would pave the way for high-silica CHA zeolite membranes to practical natural gas upgrading.

Supporting Information

The Supporting Information contains detailed experimental procedures, additional Tables S1-S4, and Figures S1-S19. The authors have cited additional references within the Supporting Information.[45]

Acknowledgements

This work is sponsored by the National Key Research and Development Program of China (2021YFC2101200), the National Natural Science Foundation of China (22178164, 22035002, 22378187), Jiangsu Provincial Carbon Peak Carbon Neutral Science and Technology Innovation Special Fund (BE2022033), Jiangsu Specially-Appointed Professors Program, State Key Laboratory of Materials-Oriented Chemical Engineering (ZK202002), Postgraduate Research & Practice Innovation Program of Jiangsu Province (KYCX23_1474).

Conflict of Interest

The authors declare no conflict of interest.

Data Availability Statement

The data that support the findings of this study are available from the corresponding author upon reasonable request.

Keywords: membranes · gas separation · zeolites · natural gas · carbon dioxide

[1] R. Simancas, A. Chokkalingam, S. P. Elangovan, Z. Liu, T. Sano, K. Iyoki, T. Wakihara, T. Okubo, *Chem. Sci.* **2021**, *12*, 7677–7695.
[2] T. Kyotani, H. Richter, *Membranes* **2022**, *12*, 176.
[3] a) C. Algieri, E. Drioli, *Sep. Purif. Technol.* **2021**, *278*, 119295; b) F. Kapteijn, X. Wang, *Chem. Ing. Tech.* **2022**, *94*, 23–30.
[4] N. Rangnekar, N. Mittal, B. Elyassi, J. Caro, M. Tsapatsis, *Chem. Soc. Rev.* **2015**, *44*, 7128–7154.
[5] P. Du, Y. Zhang, X. Wang, S. Canossa, Z. Hong, G. Nénert, W. Jin, X. Gu, *Nat. Commun.* **2022**, *13*, 1427.
[6] S. Yang, B. Min, Q. Fu, C. W. Jones, S. Nair, *Angew. Chem. Int. Ed.* **2022**, *61*, e202204265.
[7] X. Wang, T. Zhou, P. Zhang, W. Yan, Y. Li, L. Peng, D. Veerman, M. Shi, X. Gu, F. Kapteijn, *Angew. Chem. Int. Ed.* **2021**, *60*, 9032–9037.
[8] Z. Li, J. Li, H. Rong, J. Zuo, X. Yang, Y. Xing, Y. Liu, G. Zhu, X. Zou, *J. Am. Chem. Soc.* **2022**, *144*, 6687–6691.
[9] a) S. Li, J. L. Falconer, R. D. Noble, *Adv. Mater.* **2006**, *18*, 2601–2603; b) Y. Li, Y. Wang, M. Guo, B. Liu, R. Zhou, Z. Lai, *J. Membr. Sci.* **2021**, *629*, 119277.
[10] S. I. Zones, Chevron Research Company, **1985**.
[11] M. A. Carreon, S. Li, J. L. Falconer, R. D. Noble, *J. Am. Chem. Soc.* **2008**, *130*, 5412–5413.
[12] H. Kalipcilar, T. C. Bowen, R. D. Noble, J. L. Falconer, *Chem. Mater.* **2002**, *14*, 3458–3464.
[13] Z. Bohström, B. Arstad, K. P. Lillerud, *Microporous Mesoporous Mater.* **2014**, *195*, 294–302.
[14] Y. Jeong, S. Hong, E. Jang, E. Kim, H. Baik, N. Choi, A. C. K. Yip, J. Choi, *Angew. Chem. Int. Ed.* **2019**, *58*, 18654–18662.
[15] L. Yu, A. Holmgren, M. Zhou, J. Hedlund, *J. Mater. Chem. A* **2018**, *6*, 6847–6853.
[16] J. Zhou, S. Wu, B. Liu, R. Zhou, W. Xing, *Sep. Purif. Technol.* **2022**, *293*, 121122.
[17] L. Yu, M. S. Nobandegani, A. Holmgren, J. Hedlund, *J. Membr. Sci.* **2019**, *588*, 117224.
[18] N. Kosinov, C. Auffret, C. Gucuyener, B. M. Szyja, J. Gascon, F. Kapteijn, E. J. M. Hensen, *J. Mater. Chem. A* **2014**, *2*, 13083–13092.
[19] I. Yarulina, J. Goetze, C. Gücüyener, L. van Thiel, A. Dikhtiarenko, J. Ruiz-Martinez, B. M. Weckhuysen, J. Gascon, F. Kapteijn, *Catal. Sci. Technol.* **2016**, *6*, 2663–2678.

[20] M. Noack, P. Kölsch, R. Schäfer, P. Toussaint, I. Sieber, J. Caro, *Microporous Mesoporous Mater.* **2001**, *49*, 25–37.
[21] S. Yang, Y. Chiang, S. Nair, *Energy Technol.* **2019**, *7*, 1900494.
[22] Y. Zheng, N. Hu, H. Wang, N. Bu, F. Zhang, R. Zhou, *J. Membr. Sci.* **2015**, *475*, 303–310.
[23] E. Jang, S. Hong, E. Kim, N. Choi, S. J. Cho, J. Choi, *J. Membr. Sci.* **2018**, *549*, 46–59.
[24] W. Huang, Z. He, B. Liu, Q. Wang, S. Zhong, R. Zhou, W. Xing, *Sep. Purif. Technol.* **2023**, *311*, 123285.
[25] Y. Jeong, S. Kim, M. Lee, S. Hong, M.-G. Jang, N. Choi, K. S. Hwang, H. Baik, J.-K. Kim, A. C. K. Yip, J. Choi, *ACS Appl. Mater. Interfaces* **2022**, *14*, 2893–2907.
[26] a) L. Yu, M. S. Nobandegani, J. Hedlund, *J. Membr. Sci.* **2022**, *641*, 119888; b) Z. Zhang, H. Liu, S. Yu, J. Zhou, B. Wang, B. Liu, R. Zhou, *Chem. Eng. Sci.* **2024**, *284*, 119452.
[27] T. Tanigawa, N. Tsunoji, M. Sadakane, T. Sano, *Dalton Trans.* **2020**, *49*, 9972–9982.
[28] a) W. Bo, S. Ren, L. You, X. Meng, Y. Ji, X. Peng, M. Zhu, C. Zhang, X. Wang, X. Gu, *J. Membr. Sci.* **2024**, *690*, 122200; b) H. Liu, X. Gao, S. Wang, Z. Hong, X. Wang, X. Gu, *Sep. Purif. Technol.* **2021**, *267*, 118611.
[29] M. Sakai, N. Fujimaki, G. Kobayashi, N. Yasuda, Y. Oshima, M. Seshimo, M. Matsukata, *Microporous Mesoporous Mater.* **2019**, *284*, 360–365.
[30] a) Y. Shinno, K. Iyoki, K. Ohara, Y. Yanaba, Y. Naraki, T. Okubo, T. Wakihara, *Angew. Chem. Int. Ed.* **2020**, *59*, 20099–20103; b) C.-R. Boruntea, L. F. Lundegaard, A. Corma, P. N. R. Vennestrøm, *Microporous Mesoporous Mater.* **2019**, *278*, 105–114.
[31] Z. Zhao, Y. Xing, S. Li, X. Meng, F.-s. Xiao, R. McGuire, A.-N. Parvulescu, U. Müller, W. Zhang, *J. Phys. Chem. C* **2018**, *122*, 9973–9979.
[32] M. Kumar, H. Luo, Y. Román-Leshkov, J. D. Rimer, *J. Am. Chem. Soc.* **2015**, *137*, 13007–13017.
[33] a) C. Peng, Z. Liu, A. Horimoto, C. Anand, H. Yamada, K. Ohara, S. Sukenaga, M. Ando, H. Shibata, T. Takewaki, R. R. Mukti, T. Okubo, T. Wakihara, *Microporous Mesoporous Mater.* **2018**, *255*, 192–199; b) X. Liu, *Front. Chem. Sci. Eng.* **2020**, *14*, 216–232.
[34] X. Wang, Y. Zhang, X. Wang, E. Andres-Garcia, P. Du, L. Giordano, L. Wang, Z. Hong, X. Gu, S. Murad, F. Kapteijn, *Angew. Chem. Int. Ed.* **2019**, *58*, 15518–15525.
[35] H. e Qiu, Y. Zhang, L. Kong, X. Kong, X. Tang, D. Meng, N. Xu, M. Wang, Y. Zhang, *J. Membr. Sci.* **2020**, *603*, 118023.
[36] J. Okazaki, H. Hasegawa, N. Chikamatsu, K. Yajima, K. Shimizu, M. Niino, *Sep. Purif. Technol.* **2019**, *218*, 200–205.
[37] Z. Cao, N. D. Anjikar, S. Yang, *Separations* **2022**, *9*, 47.
[38] M. Lee, G. Lee, Y. Jeong, W.-J. Oh, J.-g. Yeo, J. H. Lee, J. Choi, *J. Membr. Sci.* **2022**, *646*, 120246.
[39] J. M. van de Graaf, F. Kapteijn, J. A. Moulijn, *Microporous Mesoporous Mater.* **2000**, *35-36*, 267–281.
[40] J. van den Bergh, W. Zhu, J. Gascon, J. A. Moulijn, F. Kapteijn, *J. Membr. Sci.* **2008**, *316*, 35–45.
[41] S. E. Jee, D. S. Sholl, *J. Am. Chem. Soc.* **2009**, *131*, 7896–7904.
[42] R. Krishna, S. Li, J. M. van Baten, J. L. Falconer, R. D. Noble, *Sep. Purif. Technol.* **2008**, *60*, 230–236.
[43] G. Dibrov, M. Ivanov, M. Semyashkin, V. Sudin, G. Kagramanov, *Fibers* **2018**, *6*, 83.
[44] M. Lee, Y. Jeong, S. Hong, J. Choi, *J. Membr. Sci.* **2020**, *611*, 118390.
[45] a) X. Wang, M. Shan, X. Liu, M. Wang, C. M. Doherty, D. Osadchii, F. Kapteijn, *ACS Appl. Mater. Interfaces* **2019**, *11*, 20098–20103; b) T. Zhou, M. Shi, L. Chen, C. Gong, P. Zhang, J. Xie, X. Wang, X. Gu, *Chem. Eng. J.* **2022**, *433*, 133567; c) T. M. Tovar, J. Zhao, W. T. Nunn, H. F. Barton, G. W. Peterson, G. N. Parsons, M. D. LeVan, *J. Am. Chem. Soc.* **2016**, *138*, 11449–11452; d) Y. Jeong, M. Lee, G. Lee, S. Hong, E. Jang, N. Choi, J. Choi, *J. Mater. Chem. A* **2021**, *9*, 12593–12605; e) J. A. Thompson, *AIChE J.* **2020**, *66*, e16549; f) M. Fasano, T. Humplik, A. Bevilacqua, M. Tsapatsis, E. Chiavazzo, E. N. Wang, P. Asinari, *Nat. Commun.* **2016**, *7*, 12762; g) N. Wang, Z. He, B. Wang, B. Liu, W. Xing, R. Zhou, *J. Membr. Sci.* **2023**, *673*, 121452.

Manuscript received: March 28, 2024
Accepted manuscript online: May 17, 2024
Version of record online: ■■, ■■

Research Articles

Gas Separation

X. Peng, L. Chen, L. You, Y. Jin, C. Zhang, S. Ren, F. Kapteijn, X. Wang,* X. Gu* **e202405969**

Improved Synthesis of Hollow Fiber SSZ-13 Zeolite Membranes for High-Pressure CO_2/CH_4 Separation

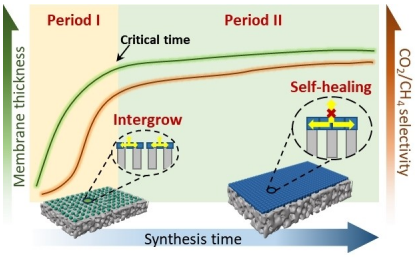

High-silica CHA zeolite is a benchmark membrane material for natural gas upgrading. The membranes were facilely synthesized by adopting the novel FAU-CHA seeds. An excellent CO_2/CH_4 separation performance was achieved even under pressure up to 6.1 MPa. The successful scaled-up synthesis paves the way for practical applications of zeolite membranes for gas separation.